AD_____

Award Number: DAMD17-02-1-0407

TITLE: Novel Role of ANX7 in Breast Cancer Progression

PRINCIPAL INVESTIGATOR: Meera Srivastava, Ph.D.

CONTRACTING ORGANIZATION: Henry M. Jackson Foundation for the Advancement of Military Medicine
Rockville, MD 20852-1428

REPORT DATE: June 2005

TYPE OF REPORT: Final

PREPARED FOR: U.S. Army Medical Research and Materiel Command
Fort Detrick, Maryland 21702-5012

DISTRIBUTION STATEMENT: Approved for Public Release;
Distribution Unlimited

The views, opinions and/or findings contained in this report are those of the author(s) and should not be construed as an official Department of the Army position, policy or decision unless so designated by other documentation.

REPORT DOCUMENTATION PAGE

Form Approved
OMB No. 074-0188

1. AGENCY USE ONLY	2. REPORT DATE	3. REPORT TYPE AND DATES COVERED
	June 2005	Final (9 May 2002 - 8 May 2005)

4. TITLE AND SUBTITLE
Novel Role of ANX7 in Breast Cancer Progression

5. FUNDING NUMBERS
DAMD17-02-1-0407

6. AUTHOR(S)

Meera Srivastava, Ph.D.

7. PERFORMING ORGANIZATION NAME(S) AND ADDRESS(ES)

Henry M. Jackson Foundation for the
Advancement of Military Medicine
Rockville, MD 20852-1428

E-Mail: msrivastava@usuhs.mil

8. PERFORMING ORGANIZATION REPORT NUMBER

9. SPONSORING / MONITORING AGENCY NAME(S) AND ADDRESS(ES)
U.S. Army Medical Research and Materiel Command
Fort Detrick, Maryland 21702-5012

10. SPONSORING / MONITORING AGENCY REPORT NUMBER

11. SUPPLEMENTARY NOTES

12a. DISTRIBUTION / AVAILABILITY STATEMENT
Approved for Public Release; Distribution Unlimited

12b. DISTRIBUTION CODE

13. ABSTRACT (Maximum 200 Words)

The purpose of this study is to determine the mechanism and the signaling pathway by which the ANX7 gene induces death of breast cancer cells. The ANX7 induced apoptotic pathway involves calcium and cytochrome c release and morphological changes, nuclear fragmentation and chromatin condensation. Down-regulation of ANX7 in nude mice inhibited the tumors and metstasis by 50% in nude mice. Additionally, we confirmed the role of calcium by determining ANX7's control on all three subtypes of IP3 Receptor expression.Overexpression of ANX7 reduces the percentage of cells that are capable of responding to the IP_3-generating agonist acetylcholine with a reduction in the magnitude of the response to acetylcholine. Using cDNA microarray and Western blot analysis, we have identified the downstream targets and signaling pathway of ANX7 in apoptosis and suppression of breast cancer cell growth. We confirmed the results that we obtained using cDNA microarray analysis, by promoter analysis and Western blot that TGF-ß1 is a downstream target for ANX7 and ANX7 activates TGF-ß1 through Smad signaling pathway regulated by calcium. These results not only establish the presence of a novel activation process following TGF-ß stimulation that requires calcium dependent ANX7-regulated activity, but also link two tumor suppressor pathways.

14. SUBJECT TERMS
ANX7, calcium, IP3 receptor, signal transduction, cDNA microarray

15. NUMBER OF PAGES
27

16. PRICE CODE

17. SECURITY CLASSIFICATION OF REPORT	18. SECURITY CLASSIFICATION OF THIS PAGE	19. SECURITY CLASSIFICATION OF ABSTRACT	20. LIMITATION OF ABSTRACT
Unclassified	Unclassified	Unclassified	Unlimited

Table of Contents

INTRODUCTION

Current attempts to develop more effective therapies for breast cancer have been focussed on the discovery of new tumor suppressor genes, in hopes of using them for gene therapy. We have recently found that the *ANX7* gene, which we discovered and have continued to study in the context of Ca^{2+} and GTP mediated exocytosis for many years (Creutz et al, 1978; ibid, 1979; Raynal and Pollard, 1994; Caohuy et al, 1996; Srivastava et al, 1996), is defective in 35% of human prostate cancer specimens (Srivastava et al., 2001) and 40% of human breast cancer specimens. A detailed analysis of ANX7 levels in hundreds of breast cancer specimens reveals that expression of this candidate tumor suppressor gene is specifically altered in primary breast cancers, ductal carcinoma in situ (DCIS) and invasive breast cancers. Furthermore, high cytoplasmic expression of *ANX7*, is a predictor of reduced disease-free survival (Srivastava et al., 2001). These data therefore, strongly suggest that the *ANX7* gene has clinical relevance for breast cancer in women. This is an important insight because until now the *ANX7* gene has never been thought to play such a role (Raynal and Pollard, 1994). In our preliminary studies with metastatic estrogen receptor positive breast cancer cells in vitro, we find that *ANX7* gene therapy causes these cells to undergo apoptosis, or programmed cell death. Therefore our **objective** in this proposal is to determine the mechanism and the signaling pathway by which the *ANX7* gene induces death of breast cancer cells. The **rationale** behind this study is the hope that such knowledge will enable us to develop therapies based on the use of the *ANX7* gene to treat or prevent breast cancer.

Our studies with both human cancer cells and the Anx7 knockout mouse have indicated the existence of a possible common deficit in calcium regulation (Srivastava et al., 1999). In the case of cancer cells, it is known that the initial signal for the onset of programmed cell death is the release of a pulse of calcium from the internal calcium stores in the endoplasmic reticulum. The calcium is released into the cytoplasm through a protein channel in the endoplasmic reticulum membrane called the IP3-Receptor. A hint regarding the possible connection between the ANX7 gene and the calcium pulse, comes from our recent work on the *ANX7* (+/-) knockout mouse. Tissues in this mouse express low levels of Anx7 protein as well as low levels of IP3-Receptors in the endoplasmic reticulum. Intracellular calcium signaling is accordingly defective, in spite of normal levels of extracellular calcium. We are reminded that apoptosis, from whatever cause, is known to be suppressed in the absence of IP3-Receptors. We also found that the effect of the anx7 gene on the DU145 prostate cancer cell line enhanced the capacity for undergoing apoptosis in the presence of staurosporine. **On the basis of these results we have hypothesized that the ANX7 gene kills breast cancer cells by increasing IP3-Receptor expression, thereby potentiating the IP3-dependent apoptotic calcium signaling pathway.**

BODY

STATEMENT OF THE THE WORK:

TIME-LINE FOR EXPERIMENTAL PLAN

	YEAR #1	YEAR #2	YEAR#3
Aim#1 and 2.			
1.a. Test sites of Ca^{2+}, GTP and PKC on ANX7 for importance in induction of apoptosis	----------		
2.a. Test tumor cells for biochemical characteristics of apoptosis		----------	
2.b. Test tumorigenicity of MCF7 cells expressing wildtype and mutant ANX7 in cancer cells			----------

Milestone #1: Elucidation of the relationship between *ANX7*-induced alteration of apoptosis and tumor suppressor activity in breast cancer cells

Milestone #2: Defining the biochemical requirements and regions in ANX7 that confer apoptosis and tumor suppressor activity in breast cancer cells

Aim #3.

3.a. Test whether ANX7 increases IP3-Receptor expression in tumor cells	----------		
3.b. Determine subcellular localization of induced IP3-Receptors		----------	
3.c. Study the physiological consequences of ANX7 expression on mobilization of intracellular Ca^{2+} in MCF7 cells expressing wildtype and mutant ANX7		----------	

Milestone #3: Investigation of mechanism by which ANX7 permits a pro-apoptotic calcium pulse to be emitted into the breast cancer cell cytosol

Aim #4.

4.a. Perform cDNA microarray studies on cells expressing wildtype and mutant *ANX7* ----------

Milestone #4: Identification of the signaling pathway by which ANX7 suppresses breast cancer cell growth

Statement of Work. 1.a.

Test sites of Ca^{2+}, GTP and PKC on ANX7 for importance in induction of apoptosis

The transformants with the 'tet off' system (from Clonetech) bearing wildtype ANX7 gene had problem of leakage in the absence of tetracycline. So we switched to adenoviral system. *ANX7* is expressed at very low levels in breast cancer cells. Hence it is critical to generate adenoviral expression vectors which has high transfection efficiency to study the biological functions of *ANX7*. To determine the involvement of calcium, GTP and PKC, we first generated mutations at those sites in mammalian pTrc99 vector and tested in vitro the ANX7 activity for membrane fusion. Therefore, we generated expression vectors containing wt-ANX7, 16 mutants against calcium binding site, 8 mutants against GTP binding site and 3 mutants against PKC binding site to study the biological functions of ANX7. The selected dominant negative mutants were reconstructed into adenovirus system and used for its activity for tumor suppression, apoptosis and IP3-Receptor expression and other downstream targets and were compared with wt-ANX7.

1.a.1. Generation of dominant negative mutants of ANX7.

Rationale: Dominant negative mutants of tumor suppressor genes have been useful for investigating the mechanism of action of these genes. Since it is well known that ANX7 forms Ca^{2+}-dependent polymers as a prelude to membrane interactions, it seemed reasonable to anticipate that mutations affecting Ca^{2+} binding might have the ability to generate partially crippled ANX7 monomers in the polymerization reaction. We reasoned that if a mutant could be found that inhibited polymerization, we could test whether tumor suppressor activity depended on this process.

Hypothesis: Mutations at some or all of the four Ca^{2+} binding sites on ANX7 may act as dominant negative mutants.

Experiment: Using standard techniques, site directed mutations were introduced into the calcium binding sites in combinations of all four crystallographically defined endonexin fold motifs. All four have the consensus sequence [GXGTDE] and the mutations were engineered to generate the amidated analogues of the charged residues (*viz.*, [GXGTNQ]). Thus we prepared 16 different combinations, including the wildtype ANX7. The combinations were single mutations (e.g., 1, 2, 3 or 4); mutations at two sites (e.g., 1 & 2, 1 & 3, etc); mutations at three sites (e.g., 1&2&3, 2&3&4,etc) and all four sites (e.g., 1&2&3&4). All the mutants were prepared and tested in the phosphatidylserine liposome fusion assay. Some were as active as the wildtype, while others were much less active. As shown in **Figure 1**, one mutant, ANX7J, was both intrinsically inactive, and profoundly inhibitory when mixed with equi-molar amounts of wildtype ANX7 (*viz.*, 1 μg each of ANX7 proteins).

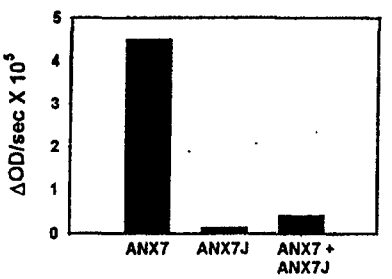

Figure 1: Dominant negative activity of ANX7J mutant when mixed with wild type ANX7 in *in vitro* membrane fusion assay.

Interpretation: ANX7J behaves as a dominant negative mutant in the *in vitro* test, and is now ready for testing for tumor suppressor activity. Inasmuch as the anx7(-/-) mouse mutant is embryonically lethal, we are prepared for the possibility that this mutation may prove to be cytotoxic.

1.a.2. Generation of GTP-binding site mutations in human anx7

Rationale: ANX7 is a Ca^{2+}-activated GTPase, which contains the five putative RAS-type canonical GTP binding sites. We reasoned that mutating these sites might allow us to test whether GTP might direct any activities of ANX7, including tumor suppression activity.

Approach: Since we did not know which mutations in these GTPase domains might be important for ANX7 activity, we created and expressed mutant ANX7's containing discrete site-directed RAS-like mutations. These sites in ANX7 were G-2 (QinT); G-4 (NRsN); and G-5 (EiSG). Binding of 8-azido-GTP could then be used to assess GTP binding.

Experiment: Mutations were generated in the putative G-2 Effector or GAP domain either as T148*A (termed TA1, mutation in the cassette exon#6), or as a double mutation,[T148*A, T148A] (termed TA2, with an additional mutation in Exon #7). Other mutations included: a G-4 mutation, N192I (termed NI in **Figure 2**); another G-4 mutation, N195D (termed ND in **Figure 2**); a G-5 mutation, L221I (termed LI in **Figure 2**). One final mutation, F233L (termed FL in **Figure 2**), a conserved site in all *ras* superfamily members, was also prepared. In *ras* this mutation disorders the GTP binding pocket.

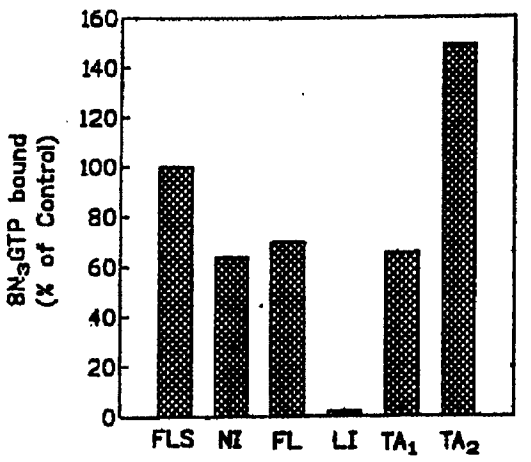

Figure 2: 8-azidoGTP photoaffinity labeling of ANX7 mutated at putative Ras-like consensus GTP-binding sites.

As shown in **Figure 2**, Western blots showed that substantial amounts of mutant proteins could be prepared. The PhosphoImager data, as well as the graphical representation below, reveal that the LI mutation entirely blocks GTP binding, while NI, TA1 and FL mutants are approximately 60% active. By contrast, the TA2 mutation is approximately 50% activated. "FLS" represents recombinant full-length synexin, or ANX7. Recall that the TA1 and TA2 mutations are in a higher molecular weight ANX7 isoform containing the cassette exon #6, and for that reason run slower on the SDS gel. In RAS, the equivalent LI mutation prevents GTP from binding, just as it does in ANX7.

Interpretation: These data serve to validate the structural basis of the intrinsic GTPase activity of ANX7, and provide mutant anx7 sequences that can be used to assess the importance of the GTPase or GTP binding for tumor suppressor gene activity.

Methods: The wildtype and mutant ANX7 proteins were expressed in the pTrc99A expression system in *E.coli*, and purified to ca. 90% by differential ammonium sulfate precipitation and column chromatography on Ultragel AcA54 (see Cauhuy et al, 1996 for more details). Specific

ANX7 content of the 47KDa or the 51KDa bands were estimated by using the ^{125}[I] anti-mouse IgG secondary antibody to label transblotted samples on nitrocellulose that had been bound by primary monoclonal antibody 10E7. ANX7 and ANX7 mutants were photolabeled by 8-N_3-^{32}[P]-GTP in the presence of 2 mM glutathione to block non-specific binding presently available in our laboratory.

1.a.3. Generation of PKC-binding site mutations in human anx7

Rationale: ANX7 is a Ca^{2+}-activated GTPase, which is activated by PKC and contains two PKC binding sites. We reasoned that mutating these sites might allow us to test whether PKC might direct any activities of ANX7, including tumor suppression activity.

Experiment: Since we did not know which mutations in these PKC binding domains might be important for ANX7 activity, we created and expressed single mutants of ANX7 in each PKC binding site and created double mutants at those sites. We measured the phosphorylation of ANX7 by PKC and found that the double mutants worked the best.

Statement of Work. 2.a.

Test tumor cells for biochemical characteristics of cell proliferation and apoptosis

Rationale: The underlying hypothesis upon which this aim is based is that the tumor suppression property can be traced to specific "hot spot" amino acid residues in the ANX7 protein. We also hypothesize that those residues that control tumor cell growth in vitro will also control tumor cell proliferation *in vivo*. To test this hypothesis we propose to begin by testing the effect of identified mutations in sites which known to affect anx7 functions such as Ca^{2+} binding, PKC binding, GTP binding and hydrolysis. For both in vitro and in vivo cases we also propose to test the effect of constructs which lead to complete loss of function, including antisense anx7 and a dominant negative anx7 mutation. If anx7 is a tumor suppressor gene, then specific residues in the ANX7 protein ought to exist which are important for the function of suppressing tumor cell proliferation and apoptosis

Approach: We have prepared ANX7 genes in a recombinant adenovirus expression system which contain tested mutations affecting different ANX7 functions. These sites include Ca^{2+} binding and GTP binding and hydrolysis. It is quite logical to anticipate that any or all of these functions might be important for suppressing the growth of tumor cells. These mutations are described in section **SOW. 1.a.** We took the dominant negative mutant ANX7J and carried out cytotoxicity assay in breast cancer cells

Experiment: Adenovirus vectors containing either the wildtype anx7 gene or the dominant negative mutant ANX7J were transfected into the non-metastatic (MDA-MB-231) and metastatic (MDA-MB-435) breast cancer cell lines and tested for growth inhibition. Initially, the cells were infected with 1, 5 or 10pfu/cell of either control adenovirus, or adenovirus expressing wildtype or mutant anx7. The cells were analyzed for their growth at different times after infection. Uninfected cells were analyzed in parallel. Cell growth was monitored and counted using a hemocytometer at 24 and 48 hours. The results which were obtained with trypan blue experiment previously reported had been carried out with adenovirus which was freeze thawed several times and was not giving reproducible results. So, we prepared and purified new batches of adenovectors containing wt-ANX7, ANX7J and p53 at the same time and stored several aliquots

in the freezer so there is no discrepancy in the results. We used p53 as a positive control. The experiments were carried out in triplicate. The cytotoxicity assay revealed that in non-metastatic 231 cells, at 24 hours wt-ANX7 and the dominant negative mutant ANX7J had similar effect, while p53 addition had begun killing the cells. However, introduction of the dominant negative mutant ANX7J or p53 killed the cells very effectively even at 1pfu at 48 hours (**Figure 3**). These results suggest that the mutation at the calcium binding site has a role to play in killing the cancer cells.

Figure 3:

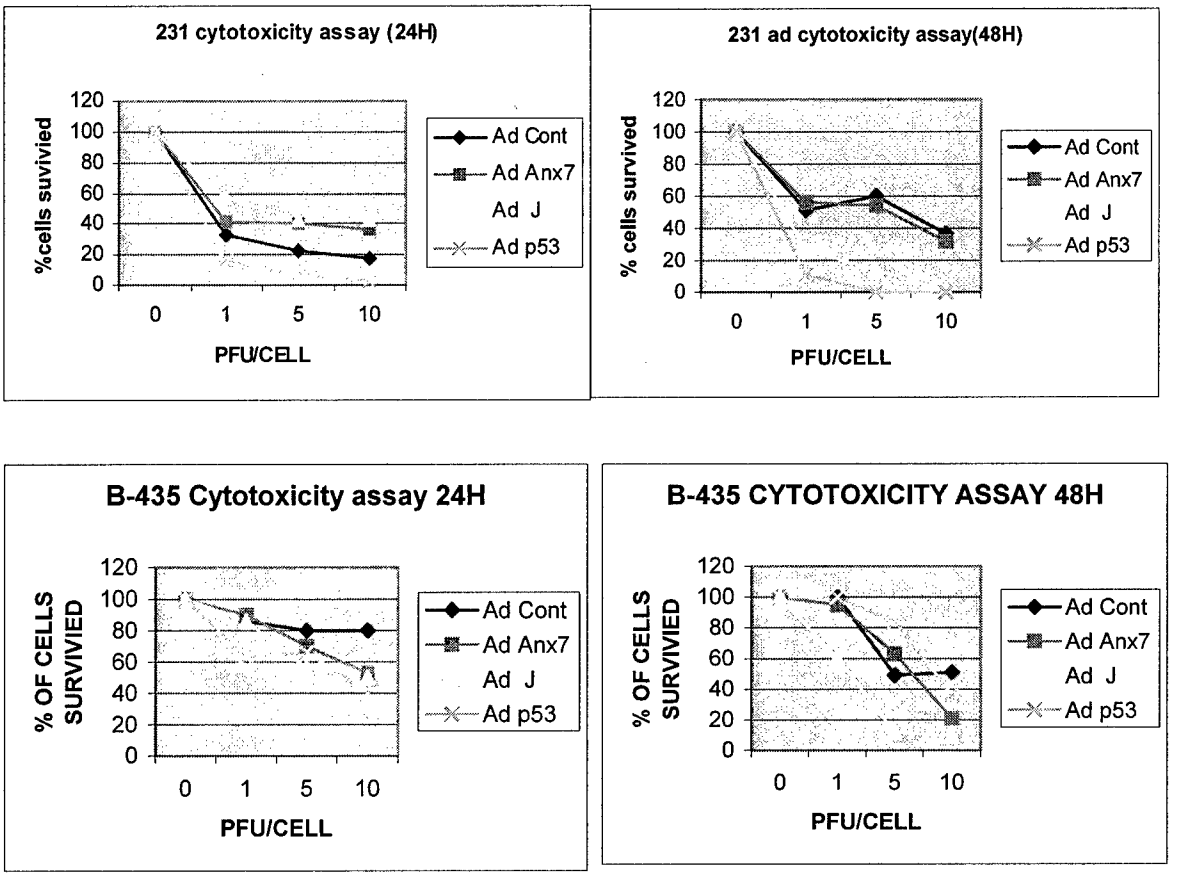

On the other hand, in the metastatic B-435 cells, at 24 hours p53 and the dominant negative mutant ANX7J behaved similarly, at 48 hours, the dominant negative mutant ANX7J killed the cancer cells effectively, while p53 did not. These results are in accordance with our finding with human clinical breast cancer specimens, since high expression of ANX7 was associated with the metastatic disease.

Interpretation: Since the dominant negative mutant ANX7J is against the calcium binding site and the addition of this mutant killed the cancer cells, we conclude that calcium associated function with this identified mutation is mechanistically involved in the tumor suppression phenotype showing metastasis. The effect of the dominant negative mutant ANX7J

in killing the cancer cells implies that down-regulation of ANX7 activity could be therapeutic for breast cancer patients

Mechanism of ANX7 induced calcium and cytochrome c release

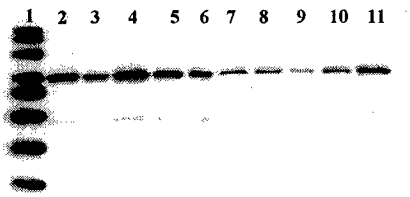

Figure 4: Western Blot of Cytochrome C release from MDA-MB-435 breast cancer cell line transfected with Ad vectors. **Lanes**: 1- MagicMark Standard, 2-6 – cytosol fractions of parental control, Ad control, AdAnx7, AdJ, AdP53 reletively, 7-11 – mitochondrial fractions of parental control, Ad control, AdAnx7, AdJ, AdP53 relatively.

Calcium elevation is a necessary preliminary event in the initiation of the apoptotic cascade (Furuya et al, 1994; Kass and Orrenius, 1999; Scoltock et al, 2000), and compounds that recruit intracellular calcium from the endoplasmic reticulum have therefore been increasingly studied as prototype drugs for induction of apoptosis in cancer cells. An example of such a compound is thapsigargin, which arrests cancer cells in G1/G0 of the cell cycle and induces the apoptotic cascade (Furuya et al, 1994; Lin et al, 1997; Tombal et al, 2000). Thapsigargin raises cytosolic Ca^{2+} concentration by blocking the SERCA-pump ATPase on the ER, thereby blocking reuptake of calcium into the ER. As a further consequence of elevation of cytosolic free calcium, either by thapsigargin or endogenous mechanisms, plasma membrane-localized store operated calcium (SOC) channels are also activated. The latter process contributes to elevation of intracellular calcium, and thus further pushes the cell into the apoptotic cascade.

Large molecules such as proteins have been shown to have similar effects to those induced by thapsigargin. For example, exogenously added TGFβ also arrests cancer cells in G1/G0, and induces apoptosis (Furuya et al, 1996). Transfection of the ANX7 gene into the cancer cells also has a very similar sequence of actions (Srivastava and Pollard, 2004). This fact, plus the high prevalence of tumors in the Anx7(+/-) knockout mouse and disorders of calcium metabolism in Anx7(+/-) mouse tissues appear to implicate a specifically thapsigargin-like mechanism for how the ANX7 gene activates human tumor cell apoptosis. For example, in cancer cells, thapsigargin raises cytosolic calcium concentration by preventing reentry of the Ca^{2+} into the ER and activates SOC channels. Similar studies of Ca^{2+} metabolism in beta cells from Anx7(+/-) knockout mice, showed that thapsigargin failed to raise cytosolic Ca^{2+}, and failed to activate SOC channels The ligand IP3 also failed to release intracellular Ca^{2+} from the ER. So, the reason for the lack of efficacy of thapsigargin in the ANX7(+/-) knockout mouse is a documented ten-fold deficiency in IP3 Receptors. (Srivastava et al, 1999). The importance of IP3 receptors in cancer cells is that IP3 Receptor activation by IP3 is the physiological stimulus needed to release calcium from the ER, thus triggering the mitochondrial permeability transition, which leads to apoptosis (Szalai, et al, 1999). We have therefore hypothesized that the action of the transfected ANX7 gene on tumor cells, may be to elevate cytosolic Ca^{2+}, and to potentiate subsequent pro-apoptotic actions of the released calcium.

Experiment: Recent studies demonstrates that calcium released from the endoplasmic reticulum synchronizes the mass exodus of cytochrome *c* from the mitochondria, a phenomenon that coordinates apoptosis. Therefore, we examined the effects of altered exogeneous *ANX7* expression on metastatic breast cancer cell line MDA-MB-435. We found that the effect of the

ANX7 gene on the MDA-MB-435 cancer cell line enhanced the release of cytochrome c by 3 fold into the cytosol in comparison to vector alone control. p53 used as a positive control increased the release of cytochrome c by only 2 fold into the cytosol (**Figure 4**).

Interpretation: The ANX7 induced apoptotic pathway involves cytochrome c release indicating the probable involvement of mitochondria

Statement of Work. 3.a.

Test tumorigenicity of MCF7 cells expressing wildtype and mutant ANX7 in cancer cells

We show that adenoviral gene transfer of DN-ANX7 suppresses breast tumorigenesis in nude mice

The effect of the dominant negative mutant ANX7J in killing the cancer cells implied that down-regulation of ANX7 activity could be therapeutic for breast cancer patients. Therefore, we used nude mice to confirm and extend the significance of this observation. we used either parental MDA-MB-435 cells harboring control adenoviral vector or MDA-MB-435 cells containing DN-*ANX7*. We evaluated for the latter cell's capacity for tumor reduction in nude mice (10 animals per group), in collaboration with our consultant, Dr. Hynda Kleinman at NIH. Parental tumor cells and their derivatives with DN-*ANX7* were cultured and harvested by tryptic digestion. Then cells were washed with serum free medium and 2 X 10^6 injected with matrigel subcutaneously in normal female athymic nude mice (6-8 weeks old). Tumor growth was followed for three weeks after the initial subcutaneous injections and growth characteristics were compared with the tumor growth rate of the parental tumor cells or the tumor cells containing control vectors. Tumor volume was determined by measuring tumor size in 3 dimensions with calipers. As shown in Figure 5, mice developed large tumors when treated with the vector alone control (**Figure 5A**). All ten mice which had DN-ANX7 (**Figure 5B**) the tumor development was reduced considerably to atleasst 66%.

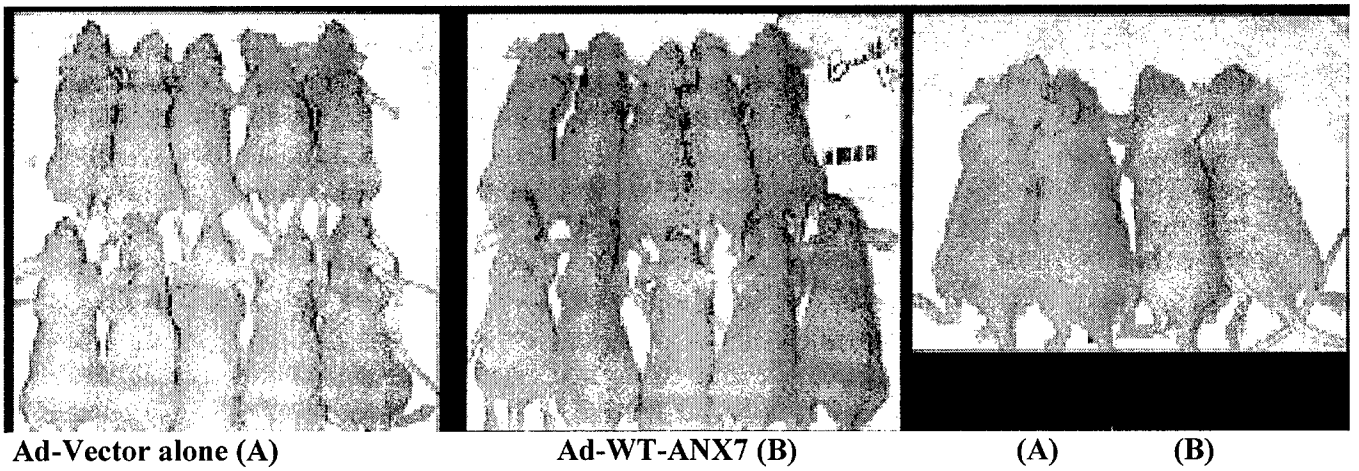

Ad-Vector alone (A) **Ad-WT-ANX7 (B)** **(A)** **(B)**

Figure 5: Effect of Ad- wt-*ANX7* towards tumor suppression in nude mice. The third column is enlarged view

B435 represents a very relevant xenograft model for tumors that metastasize. Based on data from B435 Xenograft model, nude mice was inoculated with 1-2 x 10^6 cells sub-cutaneously. Tumor size was measured every three days after tumor become visible. The end point of the study is about 6 wks after initial inoculation of cells when tumor size exceeded 2000 mm^3, calculated as: Tumor Size = length x $wide^2$ x 0.5.

After tumor reached size of 50 mm^3 a weeks time, MDA-MB-435 cells containing DN-*ANX7* administration was started by intra-tumoral injections. Three groups of animals representing control and two different dosages of the DN-ANX7 with ten animals in each group. Three animals per group per time point will be analyzed for tumor size and any metastais.

Table 1: Effect of *Anx7* Gene in distant metastasis in nude mice treated with breast cancer cells: MDA MB 435-GFP.

Animals	CONTROL								DN-*ANX7*							
Organs	1	2	3	4	5	6	7	**total**	1	2	3	4	5	6	7	**total**
Heart			6	8	33	30	3	**80**	7				5	4	6	**22**
Lung					26	50	56	**132**	3		6		18	31	27	**85**
Liver		5				5	4	**10**	6			5		3		**14**
Skull		3			3	2		**8**			1			4	1	**6**
Bone Meta																
FL one side				1				**1**	1							**1**
FL both sides		2				3		**5**								**0**
BL one side			2					**2**				1				**1**
BL both sides								**0**								**0**
FL and BL	2				4			**6**			4					**4**
Total (%)								**244** (64.7%)								**133** (35.3%)

At each weekly time tumors were harvested and scored in each organ. **Table 1** shows the effect of DN-*ANX7* Gene in distant metastasis in nude mice treated with breast cancer cells MDA MB 435-GFP. The metastasis was 53% reduced in mice treated with DN-*ANX7*. **Table 2** shows the DN-*ANX7* Gene effect on breast cancer bone metastasis which is also reduced to 50%

Table 2: The effect of DN-*ANX7* Gene in bone metastasis in nude mice treated with breast cancer cells: MDA MB 435-GFP

Bone metastasis	**Control (n=7)**	**DN- *ANX 7* (n=7)**
Frontal Legs one side	1	1
Both sides	2	0
Back Legs one side	1	1
Both sides	0	0
Frontal and back legs	2	1
Total	**6 (85.7%)**	**3(42.8%)**

These data will provide first insights into the potential of anti- ANX7 therapeutic strategy for metastatic Breast cancer and lay the foundation for clinical application.

Statement of Work. 3.a.

Test whether ANX7 increases IP3- Receptor expression in tumor cells

We show that the dominant negative ANX7 down regulated the IP3-Receptor expression in breast cancer cells

Rationale: The loss of up to 50-60% of endogenous ANX7 protein in the ANX7(+/-) knockout mouse results in a 10-fold loss of IP3 Receptors and complete loss of SOC channels. Since both IP3 Receptors and SOC channels are needed for activating apoptosis, and IP3 Receptor function is the physiological trigger for the mitochondrial permeability transition, it seems reasonable to expect that inactivating ANX7 in breast cells would down regulate IP3Receptors.

Experiment: We measured ANX7 and IP3-Receptor mRNA levels in tumor cells treated with adenovirus vector alone, wildtype and dominant negative mutant ANX7. Quantitative RT-PCR was used to quantitate the IP3Receptor messages (types 1, 2 and 3), and levels of beta-actin message was used to normalize levels of RNA used for the analyses. As is shown in **Figure 6**, dominant negative ANX7 down regulated all three IP3-Receptor expression in MCF-7 breast cancer cell line.

RT-PCR for IP3 Receptor mRNA subtypes: IP3-Receptors come in three subtypes, in which only a discrete domain varies among the three. The following HUMAN primers were prepared and tested in these experiments.

Type1= [FP:5'-CACCGCGGCAGAGATTGACAC-3'; RP: 5'-CCAGCTGCCCGGAGATTTC-3'

Type2= [FP: 5'-CTGGGGCCAACGCTAATACT-3'; RP: 5'-GAACCCCGTGATTACCTGTGACTG-3'];

Type3= [FP: 5'-GCGGGCCTGTGACACTCTACT-3'; RP: 5'-CGCCGCTCACCAGGGACAT-3'.

We found that Wt-ANX7 expression increased Ad-vector alone control from 0.49 to 0.70 and we observed corresponding increase in IP3R expression. While the dominant negative mutant ANX7J expression reached to 0.80, since it inhibited the activity of endogenous ANX7, we see a decrease in IP3R expression (**Figure 6**).

Interpretation: These results suggests that ANX7 controls all three subtypes of IP3 Receptor expression

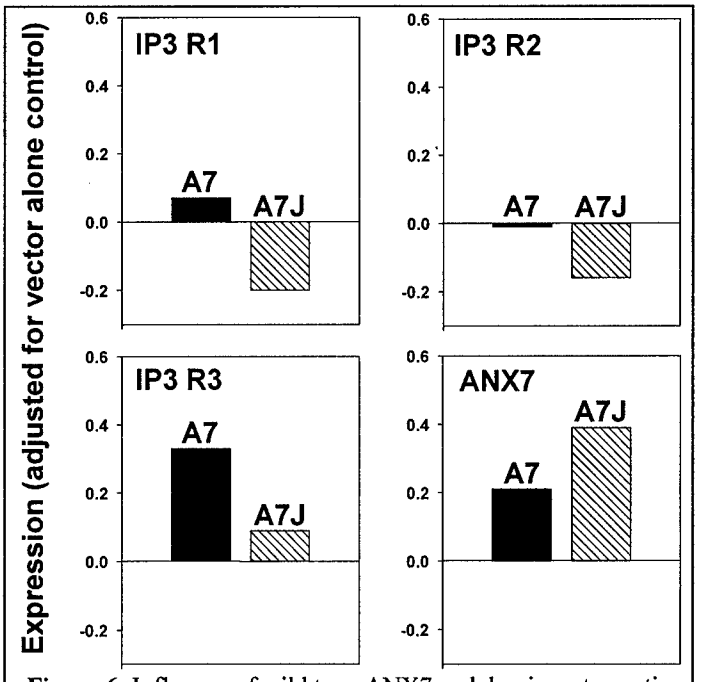

Figure 6: Influence of wild type ANX7 and dominanat negative ANX7J on IP3 Receptor subtype expression

Statement of Work. 3.b.

To determine subcellular localization of ANX7 induced IP3-Receptors

ANX7 over expression induces morphological changes and DNA fragmentation

It is possible that the morphological features may be altered in ANX7 transfected MDA-MB-435 cells compared to vector control

Experiment: The cells transfected with ANX7 were morphologically different with GFP fluorescence on the membranes and look sick. On the other hand, the GFP fluorescence is distributed throughout upon vector alone or mutant ANX7J transfection (**Figure 6**). The cell shrinkage and nuclear fragmentation can be visualized by Light microscopy with toluidine stain in ANX7 transfected cells (**Figure 7**).

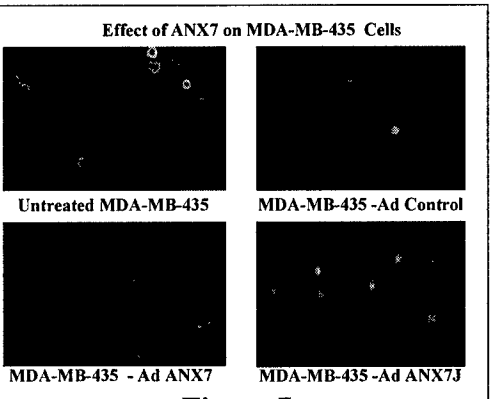

Figure 7

Interpretation: ANX7 induces morphological changes including cell shrinkage and nuclear fragmentation

EM-immunogold method to detect and quantitate ANX 7 and IP_3-Receptors.

It is possible that the anx7 or IP_3-Receptor localization and distribution to plasma membrane and nucleus may be altered in ANX7 transfected MDA-MB-435 cells compared to vector control.

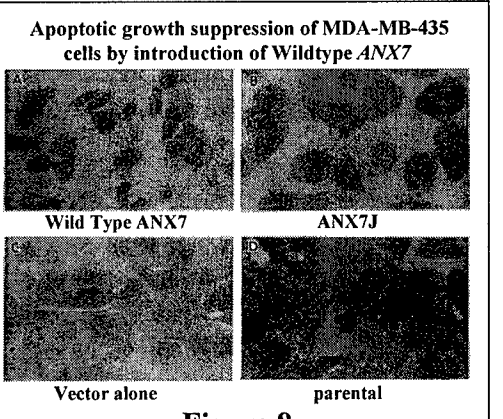

Figure 8

Experiment: we used EM-immunogold method to detect and quantitate ANX7 and IP_3-Receptors. As shown in **Figure 8**, ANX7 (large gold particles-15nm gold) and IP3 receptor (small gold particles-10nm gold) are distributed together in tumor cells not only in the plasma membrane, but also in association with secretory granule membranes. Furthermore, EM analysis revealed that ANX7 transfected cells have nuclear condensation and positive staining by TUNEL suggesting that the ANX7 gene has a role to play in inducing apoptosis (**Figure 8**).

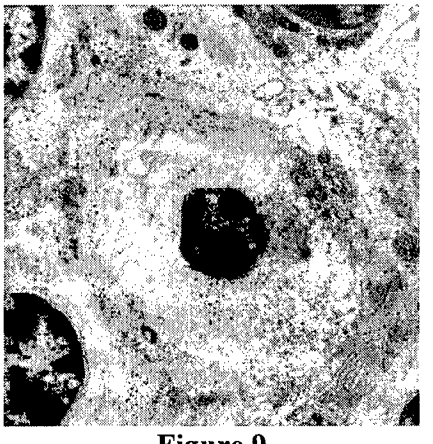

Figure 9

Interpretation: These studies reveal that while over expression of ANX7 induces apoptosis as evidenced by nuclear condensation, there is no alteration in the localization and distribution of anx7 and IP_3-Receptor expression.

Statement of Work. 3.c.

To Study the physiological consequences of ANX7 expression on mobilization of intracellular Ca^{2+} in breast cancer cells expressing wildtype and mutant ANX7

To test the hypothesis that changes in ANX7 expression levels alter Ca^{2+} homeostasis in cancer cells, we measured intracellular Ca^{2+} in MDA-MB-435 cells transfected with wt-ANX7 and the dominant-negative J mutant.

Experiement. Intracellular Ca^{2+} ($[Ca^{2+}]_i$) was measured microfluorometrically using MDA-MB-435 cells loaded with the fluorescent Ca^{2+} indicator Fura-2. Cells on glass coverslips were loaded

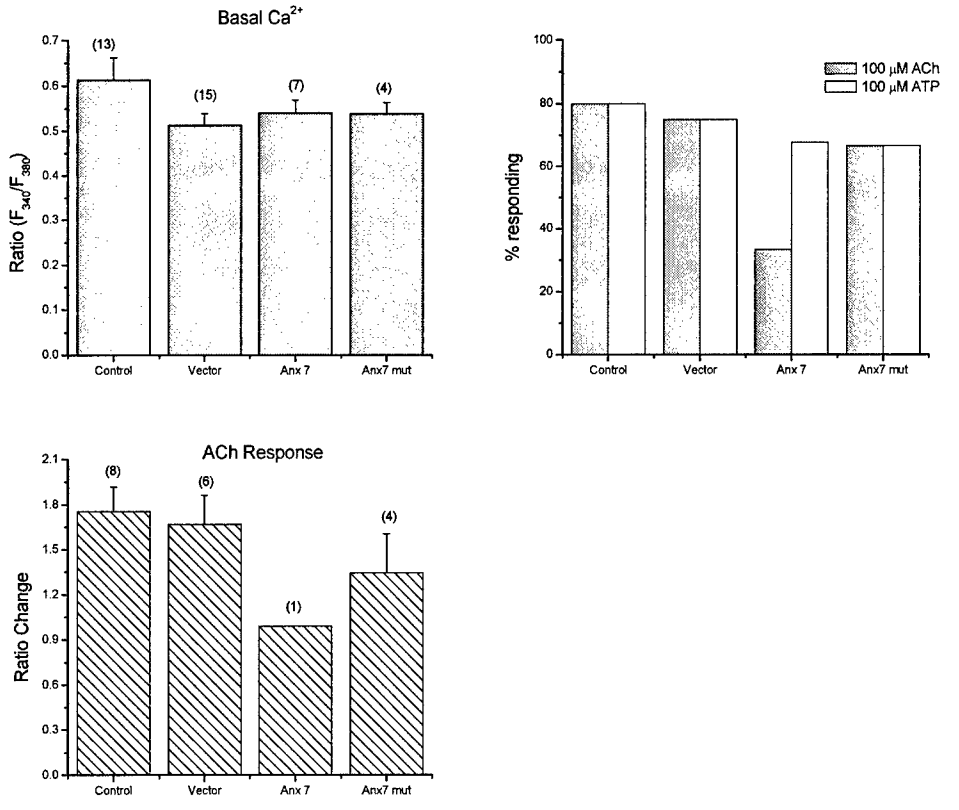

Figure 10. Effects of ANX7 expression level on intracellular Ca^{2+} in MDA-MB-435 cells. Uncalibrated intracellular Ca^{2+} ($[Ca^{2+}]_i$) measurements were made from untransfected MDA-MB-435 cells (control) and from MDA-MB-435 cells transfected with vector alone, ANX7 or J-mutant. Increase in the ratio (F_{340}/F_{380}) indicates an increase in $[Ca^{2+}]_i$. A) Average basal $[Ca^{2+}]_i$ in unstimulated cells. B) Percentage of transfected and control cells responding to the IP_3-generating agonists acetylcholine (ACh, 100 µM) and adenosine triphosphate (ATP, 100 µM) with a detectable increase in $[Ca^{2+}]_i$. C) Average magnitude of the increase in ratio (F_{340}/F_{380}) induced by 100 µM ACh in control and transfected cells.

with the membrane-permeable form of the indicator (Fura-2-AM) during a 60-minute incubation in Hank's Balanced Salt Solution containing 2 *M of the dye and 0.04% pluronic acid. The coverslips were then used to form the bottom of a sample chamber that was placed on the stage of an inverted microscope and continuously perfused with Krebs solution at 37° C. A fiber-optic based UV excitation system (DG-4, Sutter Instruments, Novato, CA) was used to excite the dye in the cells with light at 340 and 380 nm, and images of the emitted fluorescence were acquired with a digital camera under computer control. The acquisition software (Metafluor, Universal Imaging, Downingtown, PA) calculated a pixel-by-pixel ratio of the magnitude of the emitted fluorescence at the two wavelengths (F_{340}/F_{380}), which provided an uncalibrated measurement of $[Ca^{2+}]_i$. Experiments were performed 12-24 hours following transfection of the MDA-MB-435 cells.

Figure 10A shows the average basal Ca^{2+} measured from control and transfected cells (higher F_{340}/F_{380} ratio indicates higher $[Ca^{2+}]_i$). The slight decrease in basal $[Ca^{2+}]_i$ in the cells expressing the vector compared to controls likely reflects a non-specific effect of GFP on the emitted fluorescence. Expression of ANX7 or the J-mutant was not associated with changes in basal $[Ca^{2+}]_i$ when compared to the cells expressing vector alone.

To determine the effects of ANX7 expression level on the dynamics of Ca2+-sequestering intracellular stores, we measured changes in $[Ca^{2+}]_i$ caused by the IP_3-generating agonists acetylcholine (Ach) and adenosine triphosphate (ATP). We found that the majority of control cells (80%) responded to 100 *M ACh and 100 *M ATP with a rapid rise in $[Ca^{2+}]_i$ (not shown). As shown in **Figure 10B**, the percentage of responding cells was not markedly affected by expression of the vector. Interestingly, only 1 of 3 cells overexpressing ANX7 responded to Ach, while 4 of 6 cells transfected with the J mutant responded to both Ach and ATP. **Figure 10C** shows the average change in $[Ca^{2+}]_i$ induced by ACh in the various populations of cells. Expression of the vector had no effect on the response of the cells compared to controls. However, we did note that the response to ACh was markedly smaller in the single ANX7-transfected cell that responded to the agonist. The Ach-induced change in $[Ca^{2+}]_i$ was also slightly smaller in the 4 of 5 J-transfected cells that responded. No such differences were observed in the magnitude of the response of the various cell groups to ATP (not shown).

Interpretation: From these studies we are able to conclude that expression of ANX7 or the J mutant in MDA-MB-435 cells does not alter basal $[Ca^{2+}]_i$ levels. Furthermore, although these data are preliminary, they do support the hypothesis that disruption of ANX7 levels alters Ca^{2+} signaling in MDA-MB-435 cells. In particular, the data suggest that overexpression of ANX7 reduces the percentage of cells that are capable of responding to the IP_3-generating agonist acetylcholine. Furthermore, overexpression of either ANX7 or the J-mutant may be associated with a reduction in the magnitude of the response to ACh. Future studies will be carried out to increase the number of observations for statistical purposes as well as to investigate the mechanisms underlying ANX7-induced changes in Ca^{2+} responses in MDA-MB-435 cells.

Statement of Work. 4.a.

4.a.1. To identify the downstream targets of ANX7 that constitute the ANX7 signaling pathway by which ANX7 causes apoptosis and suppresses breast cancer cell growth.

Rationale: To investigate the underlying genomic mechanisms of wt-Anx7 action in breast cancer cells, we examined gene expression in breast cancer cells using cDNA microarrays obtained from clonetech. Our hypothesis is that we can assess **the downstream targets and signaling pathway** of ANX7 in apoptosis and suppression of breast cancer cell growth.

Experiment : In order to assess the downstream targets of ANX7 in breast cancer cells, we isolated mRNA's from parental breast cancer cells, breast cancer cell lines transfected with either vector alone, wild-type, or dominant negative mutant ANX7J. We used ATLAS^{TM} cDNA expression cancer array to obtain the expression profiles. Comparison of the transcripts between control, ANX7J and ANX7 wild type transfected tumor cells. **Table 3** shows the results of the microarray data analysis described in Methods section below, revealed the genes that are most affected by wt-*ANX7* and *p53* and least affected by *ANX7J.* On top of the lists are genes related to calcium binding (S100 calcium binding protein), apoptosis and tumor suppression (TGF-beta) and cell cycle (p19, an inhibitor of CDK4).

Interpretation: The genes associated with the tumor varied with a diverse biological/biochemical functions linked to cell proliferation, apoptosis and tumorigenesis.

Methods:

Preparation and labeling of RNA

Total RNAs from breast cancer cells, either parental or transfected with either vector alone or ANX7, or p53 as a positive control were prepared by the method of Champenski et al. and were subjected to DNAse 1 digestion to eliminate genomic DNA contamination. Two rounds of purification of poly A+ RNA from total RNA were performed using the mRNA isolation kit from Invitrogen as recommended by the manufacturer. The quality of the RNA were tested by running a formaldehyde denatured agarose gel and quantitated by measuring the optical density at 260nm. A

Table 3: List of genes that are most affected by *ANX7* and *p53* and least affected by *ANX7J*

Gene	parental	Vector alone	ANX7	Anx7J	P53
S100 calcium binding protein A4 (calcium protein, calvasculin, metastasin, murine placental homolog)	0.916	0.961	0.586	0.967	0.564
splicing factor, arginine/serine-rich 7, 35kDa	0.031	0.230	-0.059	0.200	-0.128
c-mer proto-oncogene tyrosine kinase	0.068	-0.296	-0.034	-0.290	-0.253
KIAA0303 protein	0.031	-0.296	-0.034	-0.253	-0.061
immunoglobulin heavy constant gamma 3 (G3m marker)	1.111	2.638	0.881	1.864	2.098
proteasome (prosome, macropain) activator subunit 1 (PA28 alpha)	-0.108	0.060	-0.143	0.100	-0.165
transforming growth factor, alpha	-0.166	-0.296	0.073	-0.218	-0.061
TRAF interacting protein	-0.108	0.167	-0.143	0.115	-0.003
cyclin-dependent kinase inhibitor 2D (p19, inhibits CDK4)	0.521	0.861	0.364	0.622	0.384
basigin (OK blood group)	1.238	1.680	1.111	1.458	1.296
gonadotropin-releasing hormone receptor	0.165	0.447	0.033	0.392	0.337
interleukin 14	-0.081	-0.338	-0.113	-0.429	-0.003
phosphoribosylglycinamide formyltransferase, phosphoribosylglycinamide synthetase, phosphoribosylaminoimidazole synthetase	0.010	0.602	-0.010	0.358	0.298
phosphoribosyl pyrophosphate synthetase 1	0.232	0.206	-0.010	0.259	0.024
pleiotrophin (heparin binding growth factor 8, neurite growth-promoting factor 1)	-0.011	0.206	-0.113	0.200	0.191
chromogranin B (secretogranin 1)	0.232	0.565	0.109	0.340	0.208
MCM2 minichromosome maintenance deficient 2, mitotin (S. cerevisiae)	0.010	0.352	0.053	0.270	0.155
nth endonuclease III-like 1 (E. coli)	1.002	1.167	0.872	1.416	0.613
growth arrest-specific 2	-0.233	-0.224	0.142	-0.332	-0.031
ribosomal protein L13a	0.936	1.007	0.797	1.265	0.312
pleckstrin homology, Sec7 and coiled/coil domains 2-like	0.332	0.745	0.427	0.646	0.578
aryl hydrocarbon receptor	0.031	-0.259	-0.010	-0.186	-0.128
tenascin R (restrictin, janusin)	0.459	-0.083	0.354	-0.031	-0.031
ribosomal protein S6 kinase, 90kDa, polypeptide 1	0.521	0.488	0.383	0.571	0.240
B-cell growth factor 1, 12kDa	0.165	0.361	-0.010	0.312	0.325

^{32}P labeled cDNA probe was synthesized from 1 μg of poly A+ RNA from control and tumor samples using MMLV reverse transcriptase, dNTP mix and CDS primer mix comprising the oligonucleotide sequences for the 1200 cancer related genes spotted on the atlas cDNA microarray. The reaction was carried out in a thermocycler set at 50°C for 25 min. and terminated by the addition of 0.1M EDTA, pH 8.0 and 1mg/ml glycogen. The ^{32}P labeled cDNA probe was then purified from unincorporated ^{32}P labeled nucleotides by using a CHROMA SPIN-200 column (clonetech) as recommended by the manufacturer. The human atlas cDNA expression array containing 1200 cancer related genes on a nylon membrane was prehybridized using Express Hyb (clonetech) at 68°C for 1 hr and hybridized overnight at 68°C with the denatured and neutralized ^{32}P labeled cDNA probe. The membrane was washed three times with 2 X SSC, 1% SDS at 68°C for 30 min. each and twice with 0.1% SSC, 0.5% SDS at 68°C for 30 min. each. The atlas array will be exposed overnight and the results will be compared with the known distribution of genes.

Imaging and quantitation of the cDNA microarray: Imaging data from the Storm PhosphorImager were downloaded into a Microsoft Excel spreadsheet. Duplicate data points were ratio'ed to the ubiquitin standard. Data were then analyzed using the Stanford University ScanAlyze software. These data were also evaluated in parallel with the PSCAN program for point identification and with the JMP program for graphical organization.

Statistical Data mining from cDNA arrays: The first strategy we employed is embodied in the GRASP methodology (Gene Ratio AnalysiS Paradigm, Srivastava et al, 1999). The GRASP algorithm allows us to specify the changes in specific intensities of given genes which are greater or less than one standard deviation (S.D.) from the average changes of all genes in the entire array. This technique vastly increases the statistical power of the analysis.

4.a.2. Analysis of members of the ANX7 signaling pathway involved in suppression of breast cancer cell growth and apoptosis using protein specific antibodies and Western blot analysis

Rationale: In order to follow the signaling pathway for Anx7 action in breast cancer cells, we investigated the effect of wt-Anx7 on the proteins that are specifically involved in apoptosis using commercially available antibodies against the known proteins. The role of calcium was examined using the dominant negative mutant, ANX7J.

Experiment: Cell extracts were prepared from breast cancer cell lines and cells transfected with 1.0 or 2.0 μg of pAd-CMV (control), ANX7 and ANX7J. Briefly, the cell pellet was resuspended in 200 μl extraction buffer containing 20 mM HEPES (pH 7.9), 0.42 M NaCl, 1.5 mM MgCl2, 0.2 mM EDTA, 0.5 mM DTT, 25% glycerol and protease inhibitor cocktail (Roche, Lewes, UK) and incubated on ice for 30 min with intermittent mixing. The extract was centrifuged for 20 min at 4°C at 10,620*g*. The supernatant was directly used for Western blot analyses. Proteins were separated on a 10% SDS-polyacrylamide gel and transferred electrophoretically to a Sequi-Blot PVDF membrane (Bio-Rad) in 20 mM sodium phosphate buffer (pH 6.8). The filter was blocked in 5% BSA in TST, washed in TST buffer alone and incubated at room temperature for 1.5 hr with the respective antibody specific for the proteins that are shown in **Table 4** at the recommended dilution. The filter was washed in TST and incubated with a 1:10,000 dilution of second antibody HRP conjugate. After extensive washing in TST, the blot was incubated with

Table 4: Proteins affected by altered expression of *ANX7* or *P53*

	MDAMB-435 Cells					MDAMB-231 Cells				
Protein	***parental***	***control***	***ANX7***	***J***	***P53***	***parental***	***control***	***ANX7***	***J***	***P53***
PARP: Poly(ADP-ribose) polymerase	-	-	-	-	-	-	-	-	-	-
RIP: Receptor Interacting Protein	-	-	-	-	-	-	-	-	-	-
FAS: Factor activating exoenzyme	n.d.	n.d.	n.d.	n.d.	n.d.	n.d.	n.d.	n.d.	n.d.	n.d.
BCL-2: B cell leukemia/lymphoma protein2	-	-	-	-	-	-	-	-	-	less
Cas: Cellular Apoptosis Susceptibility gene	-	-	-	-	-	-	-	-	-	less
P53: tumor suppressor gene	-	-	-	less	over	-	-	over	over	over
Casp3: Caspase3	-	-	-	-	-	-	-	less	over	less
GAPDH: glyceraldehyde3-phosphate dehydrogenase	over	over	over	over	over	-	-	-	-	-
Casp2: Caspase 2	-	-	-	-	-	-	-	-	-	less
Casp7: Caspase 7	-	-	-	-	less	-	-	-	-	less
BAX: BCL2 associated X protein	-	-	-	-	-	-	-	-	-	-
TRADD: TNFR-1associated death domain protein	-	-	-	-	-	-	-	-	-	-
BAD: Cell death repressor	-	-	over	-	-	n.d.	n.d.	n.d.	n.d.	n.d.
DFF45: DNA fragmentation factor	-	-	-	-	-	-	-	-	-	less
NIP1: Bd family protein	-	-	-	-	-	-	-	-	-	-
MCL-1: Myeloid cell leukemia protein	n.d.	n.d.	n.d.	n.d.	n.d.	n.d.	n.d.	n.d.	n.d.	n.d.
hILP: Human IAP-like protein	-	-	-	-	-	-	-	over	over	less
FADD: Apoptosis associated protein	-	over	less	less	over	-	over	-	-	less
Cyclin E: Cycline E	-	-	-	-	-	-	-	over	over	less
Fas ligand: Factor activating exoenzyme ligand	-	-	-	-	-	-	over	over	over	less
BCL-X: Apoptosis regulator	less	over	-	-	-	less	less	over	over	less
Apaf1: Apoptotic protease-activating factor1	-	-	-	less	-	-	less	less	less	-
ANX7: Annexin VII	-	-	over	-	-	-	-	over	over	less

n.d.: not detected; - no change in expression

SuperSignal West Pico Chemiluminescence kit (Pierce, Rockford, IL) reagents and exposed to XAR .lm.

The results show that altered ANX7 has differential effects on p53 protein, caspase-3, BAD, FADD an apoptosis associated protein, cyclin E, Fas ligand, BCLX, APAF-1 in the metatsatic and non-metastatic breast cancer cells

Interpretation: We have identified several proteins that are involved involved with apoptosis differentially expressed in the wt-ANX7 transfected tumor cells compared to the dominant negative mt-ANX7J using western blotting.

Statement of Work. 4.a. (Second year)

To identify the downstream targets of ANX7 that constitute the ANX7 signaling pathway by which ANX7 causes apoptosis and suppresses breast cancer cell growth.

Rationale: To investigate the underlying genomic mechanisms of wt-Anx7 action in breast cancer cells, we examined gene expression in breast cancer cells using cDNA microarrays obtained from clonetech. We assessed **the downstream targets and signaling pathway** of ANX7 in apoptosis and suppression of breast cancer cell growth in the last year. In this year we compared gene expression in breast cancer cells with gene expression in normal cells and asked the question which of the aberrantly expressed genes have been brought back to its normal expression by the addition of *ANX7, ANX7J* or p53

Experiment : In order to assess these targets of ANX7 or p53 in breast cancer cells, we isolated mRNA's from normal breast epithelial cell line 184B5, parental breast cancer cells, breast cancer

cell lines transfected with either vector alone, wt-*ANX7*, dominant negative mutant *ANX7J* or p53 used as a positive control. Three breast cancer cell lines were used. Two non-metastatic adenocarcinoma cell lines such as MDA-MB-231 and MCF7 and a metastatic cell line MDA-MB-435 were used fro transfection with either vector alone, wt-*ANX7*, dominant negative mutant *ANX7J* or p53. We used ATLAS™ cDNA expression **cancer** array to obtain the expression profiles. Comparison of the transcripts between parental, *ANX7J*, wt-*ANX7* or p53 transfected tumor cells with normal breast epithelial cell line was carried out by GRASP algorithm.

Table 5: List of genes that are most affected by wt-*ANX7*, mutant *ANX7J* and *p53*

ID	non-metastatic vct / 184B5pt	435vct / 184B5pt	435A7j / 184B4pt	435Anx7 / 184B4pt	435P53 / 184B4pt
non-metastatic cells 1, protein (NM23A) expressed in	1.27	0.35	1.01	0.91	1.28
TNF receptor-associated factor 3	2.47	0.48	1.00	0.88	0.95
interferon, alpha-inducible protein 27	1.19	2.01	1.01	1.30	1.21
sialyltransferase 4A (beta-galactoside alpha-2,3-sialyltransferase)	0.88	2.50	1.03	0.87	1.00
preferentially expressed antigen in melanoma	1.24	3.25	0.94	0.62	0.93
CD9 antigen (p24)	1.01	2.27	1.04	0.93	0.85
PI-3-kinase-related kinase SMG-1	1.29	1.94	0.98	1.01	1.04
protein tyrosine phosphatase, non-receptor type 2	0.68	0.67	1.00	1.20	1.09
interferon induced transmembrane protein 2 (1-8D)	1.48	4.10	1.13	1.15	1.11
microsomal glutathione S-transferase 2	1.99	2.60	1.08	1.02	1.12
cyclin E1	1.19	2.58	1.08	1.20	1.19
protein phosphatase 1G (formerly 2C), magnesium-dependent, gamma isoform	0.97	0.50	0.96	0.86	0.79
xeroderma pigmentosum, complementation group C	0.88	1.63	0.98	1.20	1.75
caspase 6, apoptosis-related cysteine protease	0.86	2.71	1.09	1.27	1.58
major histocompatibility complex, class II, DO alpha	0.90	2.62	1.09	1.05	0.86
bone morphogenetic protein 6	1.02	1.47	1.01	1.79	1.11
X-ray repair complementing defective repair in Chinese hamster cells 1	2.46	0.55	1.04	2.54	1.22
neurotrophic tyrosine kinase, receptor, type 1	2.16	1.41	1.01	0.80	0.67
interferon consensus sequence binding protein 1	1.17	1.33	1.00	1.66	1.47
WEE1 homolog (S. pombe)	0.76	0.77	1.00	1.06	1.33
non-metastatic cells 3, protein expressed in	1.26	1.37	1.01	1.13	0.98
macrophage migration inhibitory factor (glycosylation-inhibiting factor)	1.14	2.02	1.07	1.14	0.86
Rho GDP dissociation inhibitor (GDI) alpha	1.51	0.47	1.08	1.29	1.78
hypoxia-inducible factor 1, alpha subunit (basic helix-loop-helix transcription factor)	0.45	0.47	1.09	1.21	1.28
PTK7 protein tyrosine kinase 7	1.31	2.16	1.10	1.29	1.12
jagged 1 (Alagille syndrome)	1.10	2.56	1.13	1.25	1.17
cyclin-dependent kinase 5	0.69	0.58	1.06	0.76	1.18
frizzled homolog 9 (Drosophila)	1.09	1.93	1.08	1.24	1.16
delta-like 1 homolog (Drosophila)	2.07	1.73	0.94	0.93	0.85
interferon stimulated gene 20kDa	1.67	2.97	1.18	1.20	0.92

Table 5 gives the list of genes in metastatic 435 cells whose expression levels were most corrected towards the respective expression levels in normal 184B5 breast cell line by the effect of *ANX7J*, wt-*ANX7* and P53. The genes are ordered according to our list of priorities for validating their involvement in wt-*ANX7* induced effects on breast cancer progression. These data are shown graphically in **Figure 11**, which shows the expression levels in 435 cells (as log ratio to expression in 184B5 normal breast cell line) after treatment with *ANX7J*, wt-*ANX7*, P53 or vector alone. The x-axis shows the average expression level of the respective genes in the non-metastatic 231 and MCF7 cells which appear on the diagonal as cyan points. Control 435 cells treated with vector alone are shown in magenta and the transfected cells are depicted with empty circles (for *ANX7J*), green X (for wt-*ANX7*) and blue triangles (for P53). The improvement in the expression levels is shown by the movement of the expression in the transfected cells towards the x-axis. The movement of a gene towards the x-axis means that it tends to show equivalent relative expression in 184B5 normal cells and transfected metastatic 435 cancer cells with *ANX7J*, wt-*ANX7* or P53.

Interpretation: The data thus indicate that ANX7 or p53 treatment of metastatic 435 cells makes them greatly resemble 184B5 normal cells. There is not much difference between *ANX7J* and wt-*ANX7* transfection in correcting the aberrant gene expression in cancer cells. This means that we need to use other mutants against GTP and PKC or combination of these in order to differentiate the requirements of ANX7 action. On top of the lists are genes related to apoptosis and tumor suppression (caspase 6 and TNF receptor associated factor 3) and cell cycle (Cyclin E1), and metastasis (NM23A, BMP-6).

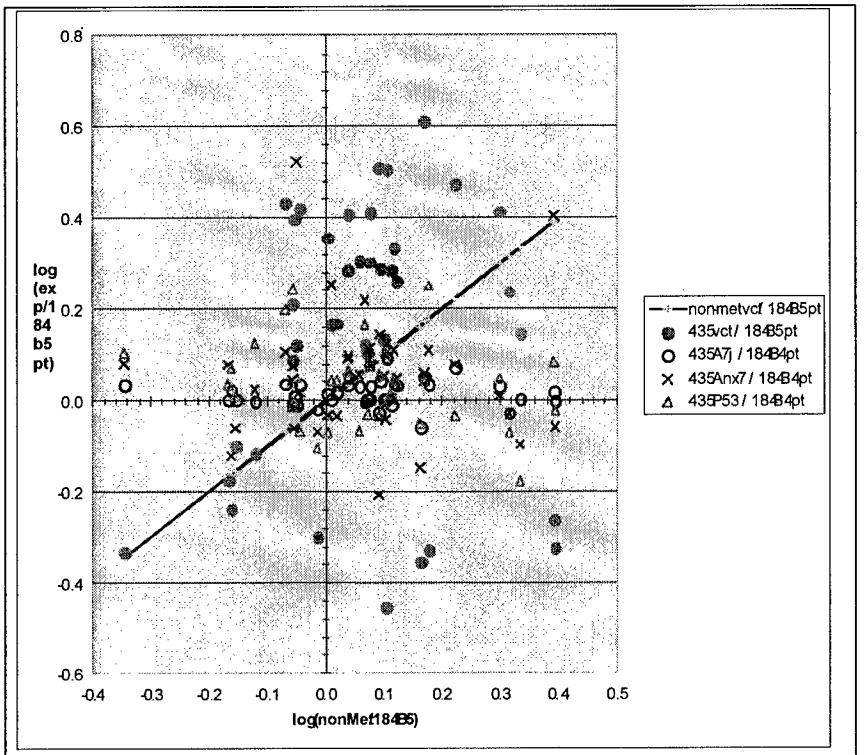

Figure 11: Expression levels in 435 cells (as log ratio to expression in 184B5 normal breast cell line) after treatment with *ANX7J*, wt-*ANX7*, P53 or vector alone.

Methods:

Preparation and labeling of RNA

Total RNAs from breast cancer cells and normal cells transfected with either vector alone or ANX7, ANX7J or p53 as a positive control were prepared by the method of Champenski et al. and were subjected to DNAse 1 digestion to eliminate genomic DNA contamination. Two rounds of purification of poly A+ RNA from total RNA were performed using the mRNA isolation kit from Invitrogen as recommended by the manufacturer. The quality of the RNA were tested by running a formaldehyde denatured agarose gel and quantitated by measuring the optical density at 260nm. A ^{32}P labeled cDNA probe was synthesized from 1 μg of poly A+ RNA from control and tumor samples using MMLV reverse transcriptase, dNTP mix and CDS primer mix comprising the oligonucleotide sequences for the 1200 cancer related genes spotted on the atlas cDNA microarray. The reaction was carried out in a thermocycler set at 50°C for 25 min. and terminated by the addition of 0.1M EDTA, pH 8.0 and 1mg/ml glycogen. The ^{32}P labeled cDNA probe was then purified from unincorporated ^{32}P labeled nucleotides by using a CHROMA SPIN-200 column (clonetech) as recommended by the manufacturer. The human atlas cDNA expression array containing 1200 cancer related genes on a nylon membrane was prehybridized

using Express Hyb (clonetech) at 68°C for 1 hr and hybridized overnight at 68°C with the denatured and neutralized ^{32}P labeled cDNA probe. The membrane was washed three times with 2 X SSC, 1% SDS at 68°C for 30 min. each and twice with 0.1% SSC, 0.5% SDS at 68°C for 30 min. each. The atlas array will be exposed overnight and the results will be compared with the known distribution of genes.

Imaging and quantitation of the cDNA microarray: Imaging data from the Storm PhosphorImager were downloaded into a Microsoft Excel spreadsheet. Duplicate data points were ratio'ed to the ubiquitin standard. Data were then analyzed using the Stanford University ScanAlyze software. These data were also evaluated in parallel with the PSCAN program for point identification and with the JMP program for graphical organization.

Statistical Data mining from cDNA arrays: The first strategy we employed is embodied in the GRASP methodology (Gene Ratio AnalysiS Paradigm, Srivastava et al, 1999). The GRASP algorithm allows us to specify the changes in specific intensities of given genes which are greater or less than one standard deviation (S.D.) from the average changes of all genes in the entire array. This technique vastly increases the statistical power of the analysis.

Statement of Work. 4.a. (Third year)

To identify the downstream targets of ANX7 that constitute the ANX7 signaling pathway by which ANX7 causes apoptosis and suppresses breast cancer cell growth.

Rationale: We identified ANX7 regulated candidate genes related to apoptosis and tumor suppression (caspase 6 and TNF receptor associated factor 3) and cell cycle (Cyclin E1), and metastasis (NM23A, BMP-6). In addition, cDNA microarray analysis revealed up-regulation of TGF-ß1 in wt-ANX7 transfected breast tumor cells (more than two standard deviations). Since TGF-ß1 is a protein that is involved in all these processes, we examined in detail the effect of ANX7 on TGF-ß1 expression. Levels of protein expression from the transciently transfected constructs were assessed by Western blot showing that TGF-ß1 protein is up-regulated by 4 fold with the addition of wt-ANX7. These data indicate that both TGF-ß1 mRNA and protein are activated by ANX7, indicating that TGF-ß1 mRNA is a target for ANX7.

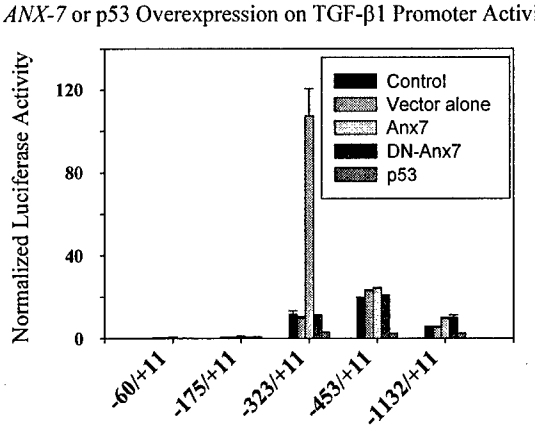

Figure 12: Effect of adenoviral vector alone, wildtype *ANX7*, dominant negative mutant of *ANX7* or p53 overexpression on TGF beta1 promoter activity

We identified the minimal region within the TGF-ß1 promoter that is regulated by ANX7

To identify the minimal region that is sufficient to bind ANX7, and confer

regulation of TGF-ß1 gene in MCF7 cells, we used a series of 5'-deletions that begins at -1132 bp and five deletion constructs downstream that ends at +11 bp in the TGF-ß1-luc construct. The expression of the luciferase gene under the control of the TGF-ß1 promoter was monitored by measuring luciferase activity. Renilla luciferase was used as an internal control to normalize the luciferase activity. The results show that introduction of adenoviral wild-type ANX7 greatly enhanced the TGF-ß-dependent activity of the luciferase reporter gene in breast cancer cell, MCF7 cells by 20-fold when compared with vector alone, p53 or dominant negative mutant of ANX7 against the calcium binding site. As shown in **Figure. 12**, this experiment mapped the elements that are contributing ANX7 induced TGF-ß1 transcription to regions of -323 bp in MCF7 cells. These experiments have the power to identify the existence of different regulatory proteins that bind to certain region and affect TGF-ß1 transcription under the control of ANX7. These results not only establish the presence of a novel activation process following TGF-ß stimulation that requires calcium dependent ANX7-regulated activity, but also link two tumor suppressor pathways.

We determined the mechanism by which ANX7 drives TGF-ß1 and induces metastatic breast cancer is through Smad signaling pathway

We have shown that *ANX7* is capable of upregulating TGF-ß1, which is often over-expressed in breast cancer. Although TGF-ß mRNA in several cancers correlates inversely with prognosis, suggesting an important paracrine role for TGF-ß in promoting tumor progression and possibly

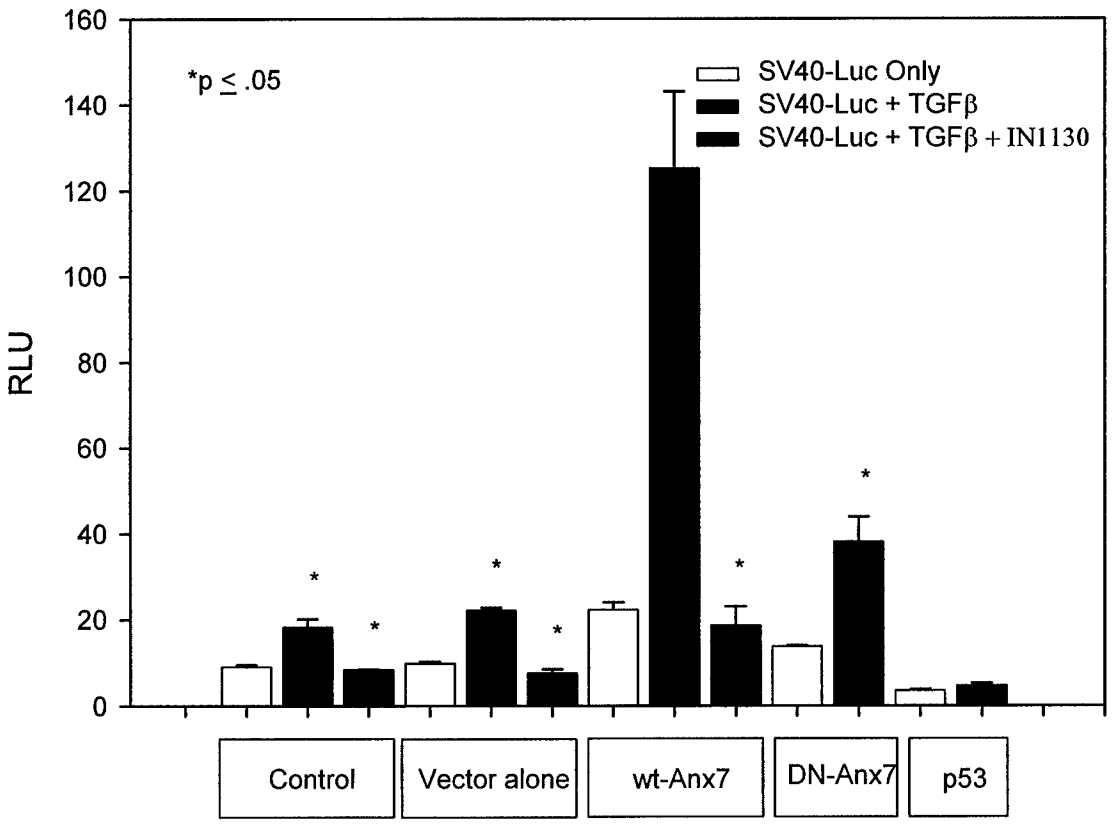

metastasis, there has been no link to date with the ANX7 tumor suppressor. Therefore, we also studied the effect of ANX7 expression on TGF-ß/Smad-dependent transcription in breast cancer cell, MDA-MB-435 cells using the Smad/TGF-ß-responsive SBE4-luc reporter construct, which contains four tandem repeats of SBE (Smad-binding element). Introduction of adenoviral wild-type ANX7 greatly enhanced the TGF-ß-dependent activity of the SBE-luc4 reporter gene in MDA-MB-435 cells by 30-fold when compared with TGF-ß alone or ANX7 transfectant alone. This induction was inhibited by 85% in MDA-MB-435 cells treated with either IN1130, a TGF-ß type I receptor inhibitor or dominant negative mutant of ANX7 against the calcium binding site.

These results not only establish the presence of a novel activation process following TGF-ß stimulation that requires calcium dependent ANX7-regulated activity, but also link two tumor suppressor pathways.

KEY RESEARCH ACCOMPLISHMENTS

AIM #1 and 2

- Generation of multi-ANX7 expression vectors for evaluation of biochemical functions of ANX7.
- Identification of the dominant negative mutant against calcium in the anx7 coding domain (DN-ANX7) which are necessary for biochemical functions of ANX7.
- Evaluation of altered ANX7 expression in breast cancer cell growth show that calcium associated function with this identified mutation is mechanistically involved in the tumor suppression phenotype and down-regulation of ANX7 could prove to be therapeutic
- The ANX7 induced apoptotic pathway involves cytochrome c release, morphological changes including cell shrinkage and nuclear fragmentation and chromatin condensation.
- Adenoviral gene transfer of DN-ANX7 suppresses breast tumorigenesis and metastasis by 50% in nude mice

AIM #3

- Evaluation of altered ANX7 expression in breast cancer cell growth shows that ANX7 controls all three subtypes of IP3 Receptor expression
- Overexpression of ANX7 or the ANX7J mutant in MDA-MB-435 cells does not alter basal $[Ca^{2+}]_i$ levels. However, overexpression of ANX7 reduces the percentage of cells that are capable of responding to the IP_3-generating agonist acetylcholine. Furthermore, overexpression of either ANX7 or the ANX7J-mutant may be associated with a reduction in the magnitude of the response to acetylcholine.

Aim #4

- We identified the apoptosis, metastatic and cell cycle "corrected" genes which show equivalent relative expression in 184B5 normal cells and transfected metastatic 435 cancer cells with *ANX7J*, wt-*ANX7* or P53.
- Identification of members of the signaling pathway of ANX7 in apoptosis and suppression of breast cancer cell growth using protein-specific antibodies and Western blot analysis
- Our studies using cDNA microarray analysis, promoter analysis and Western blot show that TGF-ß is a downstream target for ANX7 and its expression is regulated by calcium. TGF-ß is another gene that is significantly involved in apoptosis and tumor suppression.
- Introduction of adenoviral wild-type ANX7 greatly enhanced the TGF-ß-dependent activity of the SBE-luc4 reporter gene in MDA-MB-435 cells by 30-fold when compared with TGF-ß alone or ANX7 transfectant alone. This induction was inhibited by 85% in MDA-MB-435 cells treated with either IN1130, a TGF-ß type I receptor inhibitor or dominant negative mutant of ANX7 against the calcium binding site.
- These results not only establish the presence of a novel activation process following TGF-ß stimulation that requires calcium dependent ANX7-regulated activity, but also link two tumor suppressor pathways.

REPORTABLE OUTCOME

1. We showed that regulating ANX7 levels could be therapeutic. In addition, we identified the downstream targets and signaling pathway of ANX7 in apoptosis and suppression of breast cancer cell growth using cDNA microarray.
2. We showed that regulating ANX7 levels involves apoptotic events and calcium response. In addition, we identified the apoptosis, metastatic and cell cycle "corrected" genes which show equivalent relative expression in 184B5 normal cells and transfected metastatic 435 cancer cells with *ANX7J*, wt-*ANX7* or P53. for its therapeutic use.

- We showed that using cDNA microarray analysis, promoter analysis and Western blot that TGF-ß is a downstream target for ANX7 and its expression is regulated by calcium. Introduction of adenoviral wild-type ANX7 greatly enhanced the TGF-ß-dependent activity of the SBE-luc4 reporter gene in MDA-MB-435 cells by 30-fold when compared with TGF-ß alone or ANX7 transfectant alone. This induction was inhibited by 85% in MDA-MB-435 cells treated with either IN1130, a TGF-ß type I receptor inhibitor or dominant negative mutant of ANX7 against the calcium binding site.
- These results not only establish the presence of a novel activation process following TGF-ß stimulation that requires calcium dependent ANX7-regulated activity, but also link two tumor suppressor pathways.

- We sent two manuscripts and one review (**Appendix 1-3**) for publications and they are "**In Press**". A manuscript is under preparation.
- The results were presented in USUHS research day, 2003 as part of the plenary session talk and in the poster
- The results were presented in USUHS research day, 2004 as part of the plenary session talk and in the poster
- The results were also presented in the "3rd Annexin conference held in Canada, 2003 in the plenary session
- The results were also presented in the keystone symposia in colorado on the "Roles of TGF-ß in Disease Pathogenesis: Novel Therapeutic Strategies, 2005

The results formed the preliminary data for the grant, "ANX7 as a molecular target for breast cancer" that I re-submitted to NIH on March 1st

CONCLUSIONS

We have generated and identified the dominant negative mutants against calcium and GTP in the anx7 coding domain which are necessary for biochemical functions of ANX7. We have generated the effective adenoviral constructs containing the dominant negative mutants and wt-ANX7 and have shown that altered ANX7 expression during breast cancer cell growth involves calcium. The ANX7 induced apoptotic pathway involves calcium and cytochrome c release indicating the probable involvement of mitochondria. ANX7 induces morphological changes including cell shrinkage, nuclear fragmentation and chromatin condensation. Down-regulation of ANX7 in nude mice inhibited the tumororigenesis and metstasis by 50% in nude mice.

Additionally, we confirmed the role of calcium by determining ANX7's control on all three subtypes of IP3 Receptor expression. Overexpression of ANX7 or the ANX7J mutant in MDA-MB-435 cells does not alter basal $[Ca^{2+}]_i$ levels. However, overexpression of ANX7 reduces the percentage of cells that are capable of responding to the IP_3-generating agonist acetylcholine. Furthermore, overexpression of either ANX7 or the ANX7J-mutant may be associated with a reduction in the magnitude of the response to acetylcholine.

Using cDNA microarray and Western blot analysis, we have identified the downstream targets and signaling pathway of ANX7 in apoptosis and suppression of breast cancer cell growth. We identified the apoptosis, metastatic and cell cycle "corrected" genes which show equivalent relative expression in 184B5 normal cells and transfected metastatic 435 cancer cells with *ANX7J*, wt-*ANX7* or P53. We confirmed the results that we obtained using cDNA microarray analysis, by promoter analysis and Western blot that TGF-ß is a downstream target for ANX7 and its expression is regulated by calcium. Introduction of adenoviral wild-type ANX7 greatly enhanced the TGF-ß-dependent activity of the SBE-luc4 reporter gene in MDA-MB-435 cells by 30-fold when compared with TGF-ß alone or ANX7 transfectant alone. This induction was inhibited by 85% in MDA-MB-435 cells treated with either IN1130, a TGF-ß type I receptor inhibitor or dominant negative mutant of ANX7 against the calcium binding site.

Taken together, these data indicate that ANX7 suppresses breast cancer cell growth and calcium plays a role via IP3-Receptor. In addition, we have identified the members of the ANX7 signaling pathway. These results not only establish the presence of a novel activation process following TGF-ß stimulation that requires calcium dependent ANX7-regulated activity, but also link two tumor suppressor pathways.